A FIXED GRID, SHIFTED STENCIL SCHEME FOR INVISCID FLUID-PARTICLE INTERACTION

JOHN D. TOWERS

ABSTRACT. This paper presents a finite volume scheme for the scalar one-dimensional fluid-particle interaction model proposed in [F. Lagoutière, N. Seguin, T. Takahashi. A simple 1D model of inviscid fluid-solid interaction. *J. Differential Equations*, 245: 3503–3544, 2008]. When devising a finite volume scheme for this model, one difficulty that arises is how to deal with the moving source term in the PDE while maintaining a fixed grid. The fixed grid requirement comes from the ultimate goal of accommodating two or more particles. The finite volume scheme that we propose addresses the moving source term in a novel way. We use a modified computational stencil, with the lower part of the stencil shifted during those time steps when the particle crosses a mesh point. We then employ an altered convective flux to compensate the stencil shifts. The resulting scheme uses a fixed grid, preserves total momentum, and enforces several stability properties in the single-particle case. The single-particle scheme is easily extended to multiple particles by a splitting method.

Keywords. Solid-fluid interaction, Burgers equation, finite volume scheme, singular source term, moving mesh scheme, well-balanced scheme, moving interface, PDE-ODE coupling.

1. Introduction

This paper concerns a one-dimensional model of fluid-structure interaction proposed in [10]:

$$
(1.1) \quad
\begin{cases}
u_t + \partial_x(u^2/2) = \lambda\left(h'(t) - u\right)\delta(x - h(t)), & (x,t) \in \mathbb{R} \times \mathbb{R}_+ \\
mh''(t) = \lambda\left(u(h(t),t) - h'(t)\right), & t \in \mathbb{R}_+ \\
u(x,0) = u_0(x), & (h(0), h'(0)) = (h_0, v_0).
\end{cases}
$$

Here $\delta(x)$ denotes the Dirac delta measure concentrated at $x = 0$. The function $u = u(x,t)$ models the velocity of the fluid, $h(t)$ models the location of a particle at time t, $\lambda > 0$ is a drag coefficient, and $m > 0$ is the mass of the particle.

The fluid velocity is governed by the inviscid Burgers equation, and the particle-fluid coupling is due to friction, more specifically the drag term $\lambda\left(u - h'\right)$ which appears in both the PDE and the ODE in (1.1). Since there is no viscosity, the velocity $u(x,t)$ admits entropy weak solutions, meaning that shock waves occur. This leads to complex interactions between the resulting shock wave and the particle. The model is readily extended (at least formally) to accommodate multiple particles, and then there are interesting features of the solutions that include particles drafting and passing by one another.

The model (1.1) presents several conceptual and computational difficulties. First is the singular source term on the right side of the PDE in (1.1). Because there is generally a jump in the velocity u at the location of the particle $x = h(t)$, the source term is not a distribution. Next, the ODE governing the particle motion has a discontinuous right hand side. Finally, and this is the focus of the present paper, is the fact that the source term is moving. From a computational point of view, a potential method of dealing with this is to use a moving grid, so that the particle is always located at a grid cell boundary. However, it is not likely that this approach extends readily to the case where there is more than one particle, especially when the particle paths intersect. For this reason, a method that uses a fixed grid is desirable.

The model (1.1) has been studied in detail in a series of papers [1, 5, 6, 7, 10]. In [10] Lagoutière, Seguin and Takahashi provide a definition of solutions for (1.1) by studying two regularizations. They use a viscous regularization, which results in entropy inequalities, and they mollify the delta function, which leads to the proper interpretation of the nonconservative product. With these definitions in hand they completely solve the Riemann problem for (1.1), and describe the asymptotic behavior of solutions.

In [5], Andreianov, Lagoutière, Seguin and Takahashi propose a definition of entropy solution for (1.1), address the well-posedness of the problem, and introduce two finite volume methods for computing approximate solutions. One is a Glimm-like scheme, and the other is a well-balanced scheme that uses nonrectangular space-time cells near the interface. Both of the finite volume methods employ random sampling for placing the particle at a mesh interface at each time step. The nonconservative source term is handled by using a certain well-balanced scheme that was analyzed in [7]. The proper coupling of the ODE to the PDE results by enforcing a conservation of momentum principle. With these techniques they avoid the use of a moving mesh, and also avoid the use of a Riemann solver for the full model. A splitting technique is employed in order to accommodate multiple particles.

In [7], Andreianov and Seguin study in detail the model

$$(1.2) \qquad u_t + \left(u^2/2\right)_x = -\lambda u \delta(x), \quad u(x,0) = u_0(x).$$

This can be viewed as a simplification of the full model (1.1), where the particle is stationary. Its analysis is an important step in understanding (1.1), due to the presence of the nonconservative product on the right side. In order to prove existence, and for the purpose of practical computation of solutions, the authors construct a finite volume scheme, which is the one that we use as the starting point for our new scheme for (1.1). In order to establish well-posedness, the authors use the theory of conservation laws with discontinuous flux [4].

In [6], Andreianov, Lagoutière, Seguin and Takahashi prove well-posedness of the model (1.1), assuming that the initial data is of bounded variation. A wave-front tracking algorithm is used to generate approximate solutions, and among other things, a BV estimate is established for the approximations.

In [1], Aguillon, Lagoutière and Seguin propose a class of finite volume schemes for (1.1). The schemes are similar to those in [5], the important difference being that a moving grid is used, in order to keep the particle located at a fixed cell boundary. The authors are able to provide a proof of convergence to the unique entropy solution of (1.1).

Very recently, a generalized version of (1.1), where the fluid is governed by the inviscid compressible Euler equations, has been studied by Aguillon [2, 3].

In this paper we follow [5], starting from the same well-balanced scheme for (1.2), coupling the ODE to the PDE via conservation of momentum, and using a splitting method to accommodate two or more particles. Our contribution is an alternative method of handling the moving source term. We use a modified computational stencil, with the lower part of the stencil shifted during those time steps when the particle crosses a mesh point. We then employ an altered convective flux to compensate the stencil shifts. The resulting scheme uses a fixed grid, preserves the total momentum of the system, and for the single-particle model, it enforces a bound on the total variation of the solution. By testing the new scheme against Riemann problems (where the solutions are known from [10]), we find that our new scheme produces approximations that seem to converge to the correct solutions as the mesh size shrinks.

The remainder of this paper is organized as follows. In Section 2, we present our scheme for the case of a single particle, and then prove several stability properties of the scheme. In Section 3, we describe our splitting algorithm, which extends the single-particle scheme to the case of two particles. In Section 4, we describe a number of numerical experiments, the results of which indicate that our new method produces approximate solutions that are consistent with the physically relevant ones discussed in [1, 5, 6, 10]. Section 5 is a brief conclusion.

2. **Single particle**

We use a uniform spatial mesh size Δx, and temporal step size Δt^n that can be variable. Define

$$(2.1) \qquad x_j = j\Delta x,, \quad j \in \mathbb{Z}, \quad t^0 = 0, \quad t^{n+1} = t^n + \Delta t^n, \quad n \geq 0,$$

and let $\mu^n = \Delta t^n / \Delta x$. We denote by U_j^n the finite-difference approximation of $u(x_j, t^n)$, and

$$(2.2) \qquad U^n := \left(\ldots, U_{-2}^n, U_{-1}^n, U_0^n, U_1^n, U_2^n, \ldots \right), \quad \|U^n\|_\infty := \sup_{j \in \mathbb{Z}} \left| U_j^n \right|.$$

We will use the following finite difference notation:

$$(2.3) \qquad \Delta_+ U_j^n = U_{j+1}^n - U_j^n, \quad \Delta_- U_j^n = U_j^n - U_{j-1}^n.$$

We discretize the initial data according to

$$(2.4) \qquad U_j^0 := u_0(x_j-).$$

To explain our scheme, we start with the case where the particle is stationary, and located at the origin. The PDE in (1.1) then simplifies to

$$(2.5) \qquad u_t + \partial_x \left(u^2/2 \right) = -\lambda u \delta(x).$$

Let $Z_j := \lambda H(x_j)$, where $H(x)$ denotes the Heaviside function:

$$(2.6) \qquad H(x) = \begin{cases} 0, & \text{if } x \leq 0, \\ 1, & \text{if } x > 0. \end{cases}$$

As in [1] and [5], a key building block for our method is the well-balanced scheme proposed in [5] and [7] for the stationary particle model (2.5). That scheme can be
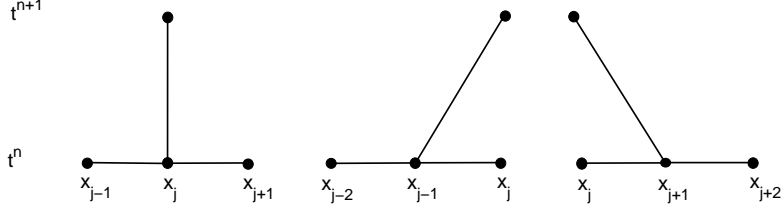
FIGURE 1. Left: the standard stencil, which is used if the particle does not cross a grid point for $t \in [t^n, t^{n+1}]$. Center: stencil when $c > 0$, and the particle crosses a grid point. Right: stencil when $c < 0$ and the particle crosses a grid point.

written in the form

$$(2.7) \qquad U_j^{n+1} = U_j^n - \mu^n \left(g(U_{j+1}^n + \Delta_+ Z_j, U_j^n) - g(U_j^n, U_{j-1}^n - \Delta_- Z_j) \right).$$

Here $g(v, u)$ is a two-point monotone numerical flux (nonincreasing with respect to v, nondecreasing with respect to u) consistent with the convective flux $f(u) := u^2/2$.

The PDE (2.5) has steady state piecewise constant solutions of the form

$$(2.8) \qquad u(x) := u_L - \lambda H(x) \text{ where } u_L \in \mathbb{R},$$

and the well-balanced scheme (2.7) preserves discrete versions of (2.8).

Now consider the case of a particle initially located at $x = 0$, moving with constant velocity c. This setup is simpler than the model (1.1), but it will suffice for the purpose of explaining how we handle the moving source term. In this case the PDE is

$$(2.9) \qquad u_t + \partial_x \left(u^2/2 \right) = -\lambda(u - c)\delta(x - ct),$$

which has piecewise constant solutions of the form

$$(2.10) \qquad u(x, t) = u_L - \lambda H(x - ct).$$

Let $Z_j^n := \lambda H(x_j - ct^n)$. A first attempt at modifying (2.7) to accommodate the moving source term of (2.9) is to simply replace Z_j everywhere in (2.7) by Z_j^n. Unfortunately, the resulting scheme does not preserve piecewise constant solutions of the form (2.10).

Our new method results by seeking to remedy this defect in as simple a manner as possible. If the particle crosses a grid point $x = x_j$ while $t \in [t^n, t^{n+1}]$, we compute U^{n+1} from the data (U^n, Z^n), as suggested in the previous paragraph, but with the data (U^n, Z^n) shifted by the amount Δx in the direction that the interface is moving. This amounts to using a modified computational stencil, with the lower part shifted as shown in Figure 1. The stencil shifts preserve the piecewise constant nature of the initial data $u_0(x) = u_L - \lambda H(x)$. However, repeatedly shifting the stencil has the cumulative effect of incorrectly translating the computed solution in

the direction opposite to the interface motion, with average speed c. We compensate for this spurious advection by replacing the convective flux $u^2/2$ by $u^2/2 - cu$.

An alternative way to view our approach is as a moving mesh method, where the mesh is only allowed to move in discrete increments of $i\Delta x$, $i \in \{-1, 0, 1\}$, so that the mesh actually never changes. Since the particle has constant speed c, the mesh is moving at an average (over many time steps) speed of c. Regarding our modified convective flux, note that it is consistent with the fact that in a standard moving mesh scheme for this problem (where the mesh moves by an amount $c\Delta t^n$ at every step), one would also replace the flux $u^2/2$ by $u^2/2 - cu$ [1].

Although the descriptions above assume a constant velocity, it turns out that a smoothly varying velocity $c(t)$, as occurs in solutions of the original model (1.1), can also be handled this way.

Let $g(v, u, c)$ denote a two-point monotone flux consistent with $f(u, c) := u^2/2 - cu$. In what follows, we will assume that the numerical flux $g(v, u, c)$ is either the Godunov numerical flux:

$$(2.11) \qquad g(v, u, c) = \begin{cases} \min_{w \in [u,v]} f(w, c), & \text{if } u \le v, \\ \max_{w \in [v,u]} f(w, c), & \text{if } v \le u, \end{cases}$$

or Enguist-Osher flux:

$$(2.12) \qquad g(v, u, c) = \frac{1}{2}\left(f(u, c) + f(v, c)\right) - \frac{1}{2}\int_u^v |f_u(w, c)|\ dw.$$

It is a standard fact about the Godunov and Engquist-Osher numerical fluxes that

$$(2.13) \qquad \min(0, f_u(v, c)) \le g_v(v, u, c) \le 0 \le g_u(v, u, c) \le \max(0, f_u(u, c)).$$

We use the following notation for the approximate particle position and its derivatives:

$$(2.14) \qquad h^n \approx h(t^n), \quad c^n \approx h'(t^n), \quad a^n \approx h''(t^n).$$

Algorithm for the single-particle model (1.1): Start with

$$(2.15) \qquad U_j^0 := u_0(x_j-), \quad h^0 = h_0, \quad c^0 = v_0, \quad Z_j^0 = \lambda H(x_j - h^0).$$

Update the the particle location and Z_j^n:

$$(2.16) \qquad h^{n+1} = h^n + c^n \Delta t^n, \quad Z_j^{n+1} = \lambda H(x_j - h^{n+1}).$$

Compute the shift index:

$$(2.17) \qquad i = i(n) := \begin{cases} 0, & \text{if } Z_j^{n+1} = Z_j^n \text{ for all } j \in \mathbb{Z}, \\ -1, & \text{if } Z_j^{n+1} \ne Z_j^n \text{ for some } j \text{ and } c^n > 0, \\ 1, & \text{if } Z_j^{n+1} \ne Z_j^n \text{ for some } j \text{ and } c^n < 0. \end{cases}$$

Then update U_j^n using the following marching formula:
$$(2.18)$$
$$U_j^{n+1} = U_{j+i}^n - \mu^n \left(g(U_{j+i+1}^n + \Delta_+ Z_{j+i}^n, U_{j+i}^n, c^n) - g(U_{j+i}^n, U_{j+i-1}^n - \Delta_- Z_{j+i}^n, c^n) \right).$$

Let $J = J(n) \in \mathbb{Z}$ denote the unique index such that $\Delta_+ Z_J^n \ne 0$. Update the acceleration and velocity via

$$(2.19) \qquad \begin{aligned} a^{n+1} &= \frac{1}{m}\left(g(U_{J+1}^n + \Delta_+ Z_J^n, U_J^n, c^n) - g(U_{J+1}^n, U_J^n - \Delta_+ Z_J^n, c^n) \right), \\ c^{n+1} &= c^n + a^{n+1}\Delta t^n, \end{aligned}$$

which completes a single iteration of the algorithm.

The following CFL condition will keep the approximate solution well behaved:

$$(2.20) \qquad \mu^n \left(\left\| U^n \right\|_\infty + \lambda + \left| c^n \right| \right) \leq 1, \quad n \geq 0.$$

We will show that if μ^n is selected in terms of the initial data so that

$$(2.21) \qquad \mu^n \left(\left\| U^0 \right\|_\infty + \lambda + \max \left(\left\| U^0 \right\|_\infty + \lambda, \left| c^0 \right| \right) \right) \leq 1,$$

then (2.20) holds for $n \geq 0$.

The first consequence of the CFL condition (2.20) is that the particle cannot move by more than Δx in the time interval $[t^n, t^{n+1}]$. This restriction, along with (2.17), implies that

$$(2.22) \qquad Z_j^{n+1} = Z_{j+i}^n, \quad \forall j \in \mathbb{Z}, \quad n \geq 0.$$

An observation contained in [10] is that for solutions (u, h) of (1.1), we should have conservation of total momentum $\mathcal{M}$, where

$$(2.23) \qquad \mathcal{M}(t) = \int_{\mathbb{R}} u(x, t)\, dx + m h'(t).$$

The discrete version of the total momentum is:

$$(2.24) \qquad M^n = \Delta x \sum_{j \in \mathbb{Z}} U_j^n + m c^n.$$

The formula (2.19) for the acceleration is designed so that the discrete total momentum will be conserved, meaning that we are coupling the ODE to the PDE via conservation of momentum, as in [1] and [5].

Proposition 2.1. *Assume that $\Delta x \sum_{j \in \mathbb{Z}} \left| U_j^n \right| < \infty$ for $n \geq 0$. Then the single-particle scheme preserves the discrete total momentum: $M^{n+1} = M^n$ for $n \geq 0$.*

Proof. Multiplying (2.18) by Δx, summing over $j \in \mathbb{Z}$, and using (2.19), we get

$$
\begin{aligned}
\Delta x \sum_{j \in \mathbb{Z}} U_j^{n+1} &= \Delta x \sum_{j \in \mathbb{Z}} U_j^n - \Delta x\, \mu^n \left(g(U_{J+1}^n + \Delta_+ Z_J^n, U_J^n, c^n) \right. \\
&\qquad \left. - g(U_{J+1}^n, U_J^n - \Delta_+ Z_J^n, c^n) \right) \\
(2.25) \qquad &= \Delta x \sum_{j \in \mathbb{Z}} U_j^n - \Delta t^n\, m\, a^{n+1} \\
&= \Delta x \sum_{j \in \mathbb{Z}} U_j^n - \Delta t^n\, m \left(\frac{c^{n+1} - c^n}{\Delta t^n} \right),
\end{aligned}
$$

from which the assertion is now immediate. $\qquad\square$

Lemma 2.1. *Assume that the CFL condition (2.20) holds. In terms of the variable $W_j^n := U_j^n + Z_j^n$, the marching formula (2.18) can be written in the following incremental form:*

$$(2.26) \qquad W_j^{n+1} = W_{j+i}^n + C_{j+i+1/2}^n \Delta_+ W_{j+i}^n - D_{j+i-1/2}^n \Delta_- W_{j+i}^n,$$

where

$$(2.27) \qquad
\begin{cases}
C_{j+1/2}^n = -\mu^n \left(\dfrac{g(U_{j+1}^n + \Delta_+ Z_j^n, U_j^n, c^n) - f(U_j^n, c^n)}{\Delta_+ (U_j^n + Z_j^n)} \right), \\[4mm]
D_{j-1/2}^n = \mu^n \left(\dfrac{f(U_j^n, c^n) - g(U_j^n, U_{j-1}^n - \Delta_- Z_j^n, c^n)}{\Delta_- (U_j^n + Z_j^n)} \right).
\end{cases}$$

The incremental coefficients satisfy

$$(2.28) \qquad 0 \leq C_{j+1/2}^n, \quad 0 \leq D_{j+1/2}^n, \quad C_{j+1/2}^n + D_{j+1/2}^n \leq 1.$$

Proof. By a straightforward algebraic manipulation, one gets

$$(2.29) \qquad U_j^{n+1} = U_{j+i}^n + C_{j+i+1/2}^n \Delta_+ W_{j+i}^n - D_{j+i-1/2}^n \Delta_- W_{j+i}^n,$$

with $C_{j+1/2}^n, D_{j+1/2}^n$ defined by (2.27). Recall that $Z_j^{n+1} = Z_{j+i}^n$, which is guaranteed by the CFL condition (2.20). The first part of the proof is then completed by adding Z_j^{n+1} to the left side of (2.29) and Z_{j+i}^n to the right side.

For the first two inequalities of (2.28), it follows directly from the monotonicity of the numerical flux $g(v, u, c)$ that $C_{j+1/2}^n, D_{j+1/2}^n \geq 0$. For the third inequality in (2.28), let us drop the superscript n. Starting from (2.27),

$$
\begin{aligned}
C_{j+1/2} &= \frac{-\mu}{\Delta_+(U_j + Z_j)} \int_0^1 \frac{d}{d\theta} g\left(U_j + \theta \Delta_+(U_j + Z_j), U_j, c\right) d\theta \\
&= -\mu \int_0^1 g_v\left(U_j + \theta \Delta_+(U_j + Z_j), U_j, c\right) d\theta \\
&\leq -\mu \int_0^1 \min\left(0, f_u(U_j + \theta\Delta_+(U_j + Z_j), c)\right) d\theta \\
&= -\mu \int_0^1 \min\left(0, U_j + \theta\Delta_+ U_j + \theta\Delta_+ Z_j - c\right) d\theta \\
&\leq -\mu \int_0^1 \min\left(0, U_j + \theta\Delta_+ U_j - c\right) d\theta.
\end{aligned}
$$

(2.30)

Here we have used (2.13), along with the fact that $\Delta_+ Z_j \geq 0$. By a similar calculation we find that

$$
\begin{aligned}
D_{j+1/2} &\leq \mu \int_0^1 \max\left(0, U_j + \theta\Delta_+ U_j - (1-\theta)\Delta_+ Z_j - c\right) d\theta \\
&\leq \mu \int_0^1 \max\left(0, U_j + \theta\Delta_+ U_j - c\right) d\theta.
\end{aligned}
$$

(2.31)

Adding (2.30) and (2.31), we get

$$
\begin{aligned}
C_{j+1/2} + D_{j+1/2} &\leq \mu \int_0^1 |U_j + \theta\Delta_+ U_j - c| \, d\theta \\
&\leq \mu \left(\max\left(|U_j|, |U_{j+1}|\right) + |c|\right).
\end{aligned}
$$

(2.32)

Finally, invoking the CFL condition (2.20), we have $C_{j+1/2} + D_{j+1/2} \leq 1$. $\qquad \square$

Proposition 2.2. *Assume that*

$$(2.33) \qquad \lambda \Delta t^n / m \leq 1,$$

and let $J = J(n) \in \mathbb{Z}$ denote the unique index such that $\Delta_+ Z_J^n \neq 0$. Then

$$(2.34) \qquad (\lambda/m)\min(0, U_{J+1}^n - c^n) \leq a^{n+1} \leq (\lambda/m)\max(0, U_J^n - c^n),$$

$$(2.35) \qquad \min\left(c^n, U_{J+1}^n\right) \leq c^{n+1} \leq \max\left(c^n, U_J^n\right).$$

Proof. Starting from the formula for a^{n+1} in (2.19),

$$
\begin{aligned}
a^{n+1} &= (1/m)\left(g(U_{J+1}^n + \lambda, U_J^n, c^n) - g(U_{J+1}^n, U_J^n - \lambda, c^n)\right) \\
&= (1/m)\int_0^1 \frac{d}{d\theta}g(U_{J+1}^n + \theta\lambda, U_J^n - (1-\theta)\lambda, c^n)\,d\theta \\
&= (\lambda/m)\int_0^1 g_v(U_{J+1}^n + \theta\lambda, U_J^n - (1-\theta)\lambda, c^n)\,d\theta \\
&\quad + (\lambda/m)\int_0^1 g_u(U_{J+1}^n + \theta\lambda, U_J^n - (1-\theta)\lambda, c^n)\,d\theta.
\end{aligned}
$$
(2.36)

With the observation that $f_u(u,c) = u - c$, and recalling (2.13), it follows that

$$
\begin{aligned}
(\lambda/m)\int_0^1 \min(0, U_{J+1}^n + \theta\lambda - c^n)d\theta &\le a^{n+1} \\
&\le (\lambda/m)\int_0^1 \max(0, U_J^n - (1-\theta)\lambda - c^n)d\theta.
\end{aligned}
$$
(2.37)

Using the fact that for $\theta \in [0,1]$,

$$
\begin{aligned}
\min(0, U_{J+1}^n - c^n) &\le \min(0, U_{J+1}^n + \theta\lambda - c^n), \\
\max(0, U_J^n - (1-\theta)\lambda - c^n) &\le \max(0, U_J^n - c^n),
\end{aligned}
$$
(2.38)

we see from (2.37) that (2.34) holds.

We now turn to the proof of (2.35). Consider two cases: $c^n \le U_J^n$ and $c^n \ge U_J^n$. First, suppose that $c^n \le U_J^n$. Then from (2.34), $a^n \le (\lambda/m)(U_J^n - c^n)$. From the velocity update formula (2.19), we then get

$$
\begin{aligned}
c^{n+1} &\le c^n + \Delta t^n(\lambda/m))(U_J^n - c^n) \\
&= (1 - (\lambda\Delta t^n/m))c^n + (\lambda\Delta t^n/m)U_J^n.
\end{aligned}
$$
(2.39)

Due to the condition (2.33), we see that $c^{n+1} \le \max(U_J^n, c^n)$. Now suppose that $c^n \ge U_J^n$. Then (2.34) implies that $a^{n+1} \le 0$, and (2.19) yields $c^{n+1} \le c^n$. In either case $c^{n+1} \le \max(U_J^n, c^n)$, and the proof of the inequality on the right in (2.35) is complete. The proof of the other half of the inequality (2.35) is similar and we omit it.

$\square$

Proposition 2.3. *Suppose that the CFL condition* (2.20) *holds at each time level. Then*

$$
\|U^n\|_\infty \le \|U^0\|_\infty + \lambda, \quad n \ge 0,
$$
(2.40)

and if the time step restriction (2.33) *also holds, then*

$$
|c^n| \le \max\left(\|U^0\|_\infty + \lambda, |c^0|\right),
$$
(2.41)

$$
\left|\frac{c^{n+1} - c^n}{\Delta t^n}\right| \le \frac{\lambda}{m}\left(\|U^0\|_\infty + \lambda + \max\left(\|U^0\|_\infty + \lambda, |c^0|\right)\right).
$$
(2.42)

In terms of the initial data, if the CFL condition (2.21) *holds, along with* (2.33), *then* (2.20) *is satisfied, again ensuring the bounds* (2.40), (2.41), *and* (2.42).

Proof. Fix a time level $n \geq 0$, and consider the time advance operator $G^n(V)$ defined by (2.18):

(2.43)
$$G^n(V)_j = G_j^n (V_{j+i+1}, V_{j+i}, V_{j+i-1})$$
$$= V_{j+i} - \mu^n \left(g(V_{j+i+1} + \Delta_+ Z_{j+i}^n, V_{j+i}, c^n) - g(V_{j+i}, V_{j+i-1} - \Delta_- Z_{j+i}^n, c^n) \right).$$

It is clear from (2.43), along with the monotonicity of the numerical flux, that G_j^n is a nondecreasing function of $V_{j+i\pm1}^n$. Also, from (2.43) and (2.13), we get

(2.44)
$$\partial G_j^n / \partial V_{j+i} \geq 1 - \mu^n \max(0, f_u(V_{j+i}, c^n)) + \mu^n \min(0, f_u(V_{j+i}, c^n))$$
$$= 1 - \mu^n |f_u(V_{j+i}, c^n)| = 1 - \mu^n |V_{j+i} - c^n|$$
$$\geq 1 - \mu^n (|V_{j+i}| + |c^n|).$$

Thus, the operator G^n will be order preserving, i.e.,

(2.45)
$$V_j \leq \hat{V}_j, \quad \forall j \in \mathbb{Z} \implies G^n(V)_j \leq G^n(\hat{V})_j, \quad \forall j \in \mathbb{Z},$$

when applied to V and $\hat{V}$ if

(2.46)
$$\mu^n \left(\|Y\|_\infty + |c^n| \right) \leq 1$$

holds for $Y = V$, $Y = \hat{V}$.

Let

(2.47)
$$U_* = \inf_{j \in \mathbb{Z}} U_j^0, \quad U^* = \sup_{j \in \mathbb{Z}} U_j^0,$$

and define

(2.48)
$$P_j^n = U_* - Z_j^n, \quad Q_j^n = U^* + \lambda - Z_j^n.$$

Since

(2.49)
$$P_j^n + Z_j^n = \text{constant}, \quad Q_j^n + Z_j^n = \text{constant},$$

it follows from Lemma 2.1, along with (2.22), that

(2.50)
$$P^{n+1} = G^n(P^n), \quad Q^{n+1} = G^n(Q^n).$$

Also, it follows from (2.48) that

(2.51)
$$\|P^n\|_\infty \leq \|U^0\|_\infty + \lambda, \quad \|Q^n\|_\infty \leq \|U^0\|_\infty + \lambda, \quad n \geq 0.$$

We focus for the moment on time level $n = 0$. From (2.48), we have the ordering

(2.52)
$$P_j^0 \leq U_j^0 \leq Q_j^0, \quad \forall j \in \mathbb{Z}.$$

This ordering will be preserved by the operator G^0 if U^0, P^0, Q^0 all satisfy the condition (2.46), which in turn will be the case if

(2.53)
$$\mu^n \left(\|U^0\|_\infty + \lambda + |c^0| \right) \leq 1,$$

which is just the CFL condition (2.20) at $n = 0$. Thus the ordering (2.52) is preserved at time level $n = 1$:

(2.54)
$$P_j^1 \leq U_j^1 \leq Q_j^1, \quad \forall j \in \mathbb{Z}.$$

Referring to (2.51), this ordering implies that

(2.55)
$$\|U^1\|_\infty \leq \|U^0\|_\infty + \lambda,$$

i.e., the bound (2.40) stated in the proposition holds at time level $n = 1$.

Now note that as a result of (2.51) and (2.55), U^1, P^1, Q^1 all satisfy the condition (2.46), and so with the ordering (2.54), we may repeat this argument, this time applying G^1. By continuing this way, the proof of (2.40) can be completed by induction.

For the proof of (2.41), note that as a result of Proposition 2.2, along with (2.40), we have

$$(2.56) \qquad \left|c^{n+1}\right| \leq \max\left(\left|c^n\right|, \left\|U^0\right\|_\infty + \lambda\right),$$

which yields (2.41) by induction.

To prove (2.42), we use (2.34) to give

$$(2.57) \qquad \left|a^{n+1}\right| \leq (\lambda/m)\left(\left\|U^n\right\|_\infty + \left|c^n\right|\right).$$

With the help of the bounds (2.40) and (2.41), along with the observation that $a^{n+1} = (c^{n+1} - c^n)/\Delta t^n$, we have (2.42).

Finally, to prove the last assertion of the proposition, we simply plug the bounds (2.40) and (2.41) into the CFL condition (2.20).

$\square$

Remark 2.1. From the last part of the proposition, it is clear that we may choose a constant $\mu^n := \mu$ once and for all based on the initial data. We leave open the possibility of variable time steps because there are situations where significantly larger time steps are possible later in the calculation than at the beginning.

Remark 2.2. The discrete L^∞ bound (2.40) is a discrete version of the L^∞ bound for the solution of the continuous problem (1.1) given by Theorem 11 of [6].

Proposition 2.4. *Suppose μ^n is chosen so that the CFL condition* (2.20) *holds, and also that the time step restriction* (2.33) *is satisfied. Then the scheme is TVD* [11] *with respect to $W^n = U^n + Z^n$:*

$$(2.58) \qquad \sum_{j\in\mathbb{Z}}\left|\Delta_+ W_j^{n+1}\right| \leq \sum_{j\in\mathbb{Z}}\left|\Delta_+ W_j^n\right|, \quad n \geq 0,$$

and we have the following total variation bound for U^n:

$$(2.59) \qquad \sum_{j\in\mathbb{Z}}\left|\Delta_+ U_j^n\right| \leq \sum_{j\in\mathbb{Z}}\left|\Delta_+ U_j^0\right| + 2\lambda, \quad n \geq 0.$$

Proof. By invoking standard results of Harten and LeRoux [8, 11, 12], the TVD property (2.58) is a direct result of the incremental form (2.26), along with (2.28).

For the proof of (2.59), we have from (2.58) that

$$(2.60) \qquad \sum_{j\in\mathbb{Z}}\left|\Delta_+ U_j^n + \Delta_+ Z_j^n\right| \leq \sum_{j\in\mathbb{Z}}\left|\Delta_+ U_j^0 + \Delta_+ Z_j^0\right|.$$

The proof is completed by applying the triangle inequality, the reverse triangle inequality, and the fact that $\sum_{j\in\mathbb{Z}}\left|\Delta_+ Z_j^n\right| = \lambda$. $\square$

Remark 2.3. The total variation bound (2.59) was proven in [1] for the moving mesh scheme of that paper, and in fact our method of proof is similar to that one. A total variation bound was proven in [6] using a wave-front tracking algorithm. The authors of [7] proved a local variation bound which, when combined with Cantor's diagonal argument, can be used instead of a total variation bound to prove compactness.

Let $\chi^n(t)$ denote the characteristic function for $[t^n, t^{n+1})$, and let $\chi_j(x)$ denote the characteristic function for $(x_j - \Delta x/2, x_j + \Delta x/2)$. Define

$$(2.61) \quad u^\Delta(x,t) = \sum_{n \geq 0} \sum_{j \in \mathbb{Z}} \chi^n(t) \chi_j(x) U_j^n, \quad h^\Delta(t) = \sum_{n \geq 0} \chi^n(t) \left(h^n + (t - t^n) c^n \right).$$

The stability results provided in Propositions 2.3 and 2.4 are sufficient for a compactness result. The following is essentially Proposition 2.4 of [1], to which we refer the reader for the proof.

Proposition 2.5. *Let $\mu^n = \mu = constant$. Suppose μ is chosen so that the CFL condition (2.20) holds, and also that the time step restriction (2.33) is satisfied. Assume that $u_0 \in BV(\mathbb{R}) \cap L^1(\mathbb{R})$. Then, modulo extraction of a subsequence, we have the following limits as $(\Delta x, \Delta t) \to (0, 0)$ with $\Delta t/\Delta x = \mu$:*

$$(2.62) \qquad\qquad u^\Delta \to u \ in \ L^1_{loc}(R \times R_+), \quad h^\Delta \to h \ in \ W^{1,\infty}_{loc}$$

for some $u \in BV(\mathbb{R}) \cap L^1(\mathbb{R})$, and $h \in W^{2,\infty}_{loc}$.

Remark 2.4. There remains the more difficult question of whether the limits u and h of the proposition above are the physically correct ones defined in [1, 5, 6, 10]. We do not address that aspect of the problem in this paper, other than to remark that our numerical experiments seem to indicate that this is the case.

3. Two particles

In this section we address the two-particle model of [5], and describe our splitting scheme for computing approximate solutions. It will become clear that the splitting scheme can be extended to any finite number of particles.

When two particles are present, the collisionless model (meaning that particles can pass through each other), is

(3.1)
$$\begin{cases} u_t + \partial_x(u^2/2) = \lambda \left(h_1'(t) - u \right) \delta(x - h_1(t)) \\ \qquad\qquad + \lambda \left(h_2'(t) - u \right) \delta(x - h_2(t)), \quad (x,t) \in \mathbb{R} \times \mathbb{R}_+ \\ m h_1''(t) = \lambda \left(u(h_1(t), t) - h_1'(t) \right), \quad m h_2''(t) = \lambda \left(u(h_2(t), t) - h_2'(t) \right), \quad t \in \mathbb{R}_+ \\ u(x, 0) = u_0(x), \quad (h_1(0), h_1'(0)) = (h_{1,0}, v_{1,0}), \quad (h_2(0), h_2'(0)) = (h_{2,0}, v_{2,0}). \end{cases}$$

To accommodate two particles, we use a splitting method, as in [5]. Since a number of splitting techniques are potential candidates [9], we describe the one that we use in some detail. We will make use of the following equivalent version of the single-particle marching formula (2.18):

(3.2)
$$\begin{cases} U_j^{n+1} = U_{j+i}^n - \mu^n \left(g(U_{j+i+1}^n, U_{j+i}^n, c^n) - g(U_{j+i}^n, U_{j+i-1}^n, c^n) \right) - \mu^n \sigma_j^n, \\ \sigma_j^n = \left(g(U_{j+i+1}^n + \Delta_+ Z_{j+i}^n, U_{j+i}^n, c^n) - g(U_{j+i+1}^n, U_{j+i}^n, c^n) \right) \\ \qquad - \left(g(U_{j+i}^n, U_{j+i-1}^n - \Delta_- Z_{j+i}^n, c^n) - g(U_{j+i}^n, U_{j+i-1}^n, c^n) \right), \end{cases}$$

and the index $k \in \{1, 2\}$ will indicate the particle number.

Algorithm for the two-particle model (3.1): Start with

$$(3.3) \qquad U_j^0 := u_0(x_j-), \quad h^{k,0} = h_{k,0}, \quad c^{k,0} = v_{k,0}, \quad Z_j^{k,0} = \lambda H(x_j - h^{k,0}).$$

Update the the particle locations and $Z_j^{k,n}$:

$$(3.4) \qquad h^{k,n+1} = h^{k,n} + c^{k,n} \Delta t^n, \quad Z_j^{k,n+1} = \lambda H(x_j - h^{k,n+1}).$$

Compute the shift indices:

$$(3.5) \qquad i^k = i^k(n) := \begin{cases} 0, & \text{if } Z_j^{k,n+1} = Z_j^{k,n} \text{ for all } j \in \mathbb{Z}, \\ -1, & \text{if } Z_j^{k,n+1} \neq Z_j^{k,n} \text{ for some } j \text{ and } c^{k,n} > 0, \\ 1, & \text{if } Z_j^{k,n+1} \neq Z_j^{k,n} \text{ for some } j \text{ and } c^{k,n} < 0. \end{cases}$$

Then compute $U_j^{k,n}$ and the source terms:

$$(3.6)$$
$$\begin{cases} U_j^{k,n+1} = U_{j+i^k}^n - \mu^n \left(g(U_{j+i^k+1}^n, U_{j+i^k}^n, c^{k,n}) - g(U_{j+i^k}^n, U_{j+i^k-1}^n, c^{k,n}) \right), \\ \sigma_j^{k,n} = \left(g(U_{j+i^k+1}^n + \Delta_+ Z_{j+i^k}^{k,n}, U_{j+i^k}^n, c^{k,n}) - g(U_{j+i^k+1}^n, U_{j+i^k}^n, c^{k,n}) \right) \\ \qquad - \left(g(U_{j+i^k}^n, U_{j+i^k-1}^n - \Delta_- Z_{j+i^k}^{k,n}, c^{k,n}) - g(U_{j+i^k}^n, U_{j+i^k-1}^n, c^{k,n}) \right), \end{cases}$$

and update the fluid velocity:

$$(3.7) \qquad U_j^{n+1} = \frac{1}{2} \left(U_j^{1,n+1} + U_j^{2,n+1} \right) - \mu^n \left(\sigma_j^{1,n} + \sigma_j^{2,n} \right).$$

Compute the acceleration and velocity of each particle:

$$(3.8) \qquad \begin{aligned} a^{k,n+1} &= \frac{1}{m^k} \sum_{j \in \mathbb{Z}} \sigma_j^{k,n}, \\ c^{k,n+1} &= c^{k,n} + a^{k,n+1} \Delta t^n. \end{aligned}$$

This completes a single iteration of the algorithm.

The two-particle version of the discrete momentum (2.24) is

$$(3.9) \qquad M^n = \Delta x \sum_{j \in \mathbb{Z}} U_j^n + m_1 c^{1,n} + m_2 c^{2,n}.$$

Proposition 3.1. *Assume that $\Delta x \sum_{j \in \mathbb{Z}} \left| U_j^n \right| < \infty$ for $n \geq 0$. Then the two-particle scheme preserves the total momentum.*

Proof. Starting from (3.7), we sum over $j \in \mathbb{Z}$, and substitute (3.6). This yields

$$(3.10) \qquad \begin{aligned} \Delta x \sum_{j \in \mathbb{Z}} U_j^{n+1} &= \Delta x \sum_{j \in \mathbb{Z}} U_j^n - \Delta x \sum_{j \in \mathbb{Z}} \left(\mu^n \sigma_j^{1,n} + \mu^n \sigma_j^{2,n} \right) \\ &= \Delta x \sum_{j \in \mathbb{Z}} U_j^n - \Delta t^n \sum_{j \in \mathbb{Z}} \left(m_1 a^{1,n+1} + m_2 a^{2,n+1} \right). \end{aligned}$$

After substituting

$$(3.11) \qquad a^{k,n+1} = \left(c^{k,n+1} - c^{k,n} \right) / \Delta t^n, \quad k = 1, 2,$$

the proof is completed in a manner similar to the proof of Proposition 2.1. $\qquad \square$

4. Numerical examples

For the numerical flux, we use the Godunov numerical flux for $g(v, u, c)$ in all examples. We use a uniform time step $\Delta t^n = \Delta t$, $\mu^n = \mu$.

Example 4.1. This is a Riemann problem, with

$$(4.1) \qquad (u_L, u_R) = (.5, -.5), \quad (h(0), h'(0)) = (0, .25), \quad \lambda = .75, \quad m = 1.$$

It is an example of Case V of Lemma 5.7 in [10]. The exact solution for the fluid velocity is piecewise constant: $u(x, t) = u_0(x - h(t))$. The approximate solution
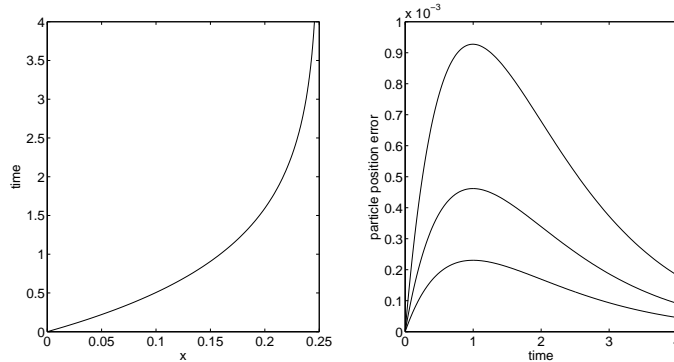
FIGURE 2. Example 4.1. Left plot: particle location. Right plot: error in particle location for $\Delta x = .04, .02, .01, \mu = .5,$
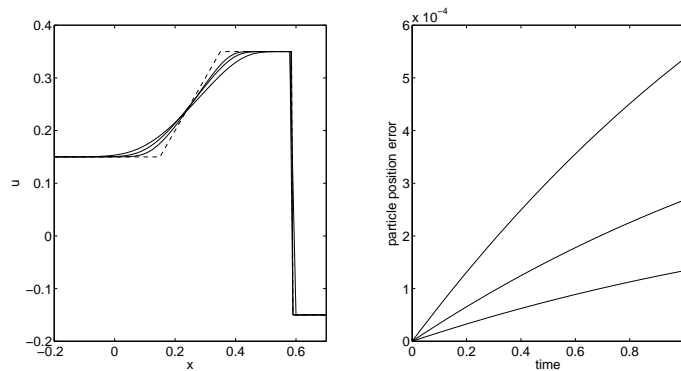

FIGURE 3. Example 4.2. Left plot: Computed and exact fluid velocity (dashed line) at $t = 1.0$ using $\Delta x = .02, .01, .005,$ and $\mu = .5$. Right plot: Error in particle location for the three mesh sizes.

is also piecewise constant. In fact, the scheme captures the fluid velocity solution exactly, except for an x-translation. The particle location is accurate to within less than one mesh width. See Figure 2.

Example 4.2. This is a Riemann problem with

$$(4.2) \qquad (u_L, u_R) = (.15, -.15), \quad (h(0), h'(0)) = (0, .65), \quad \lambda = .5, \quad m = 2.$$

It is an example of Case III of Lemma 5.7 in [10]. See Figure 3.

Example 4.3. This problem is the one in Figure 5 of [5]. We include this example for comparison. It is a Riemann problem with

$$(4.3) \qquad (u_L, u_R) = (0, -2), \quad (h(0), h'(0)) = (0.5, 15), \quad \lambda = 10, \quad m = 0.1.$$

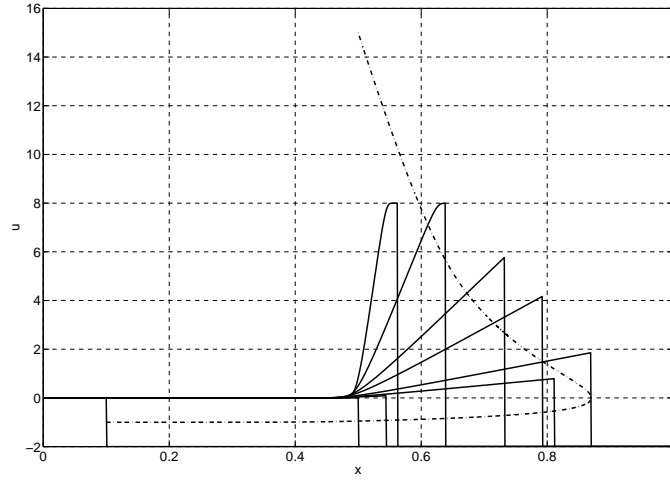We used $\Delta x = .001$, $\Delta t = 0.000025$, $\mu = .025$. See Figure 4.

FIGURE 4. Example 4.3. Solid lines: fluid velocity at times 0, 0.5×10^{-2}, 1.5×10^{-2}, 4×10^{-2}, 7×10^{-2}, 0.2, 0.4, 0.75, 1.2. Dot-dashed line: particle trajectory. (cf. Figure 5 of [5].)
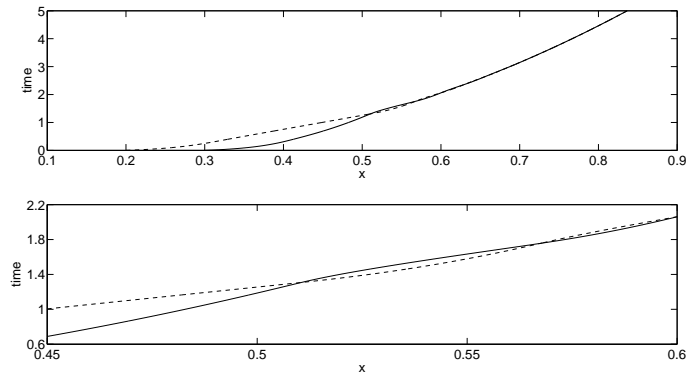

FIGURE 5. Example 4.4. Particle locations. The lower plot is a blowup of a small part of the upper plot. (cf. bottom plot of Figure 8 of [5].)

Example 4.4. There are two particles in this problem. The setup is the same as the example in Figure 8 of [5]. The data for this problem is

(4.4)
$$(h_1(0), h_1'(0)) = (0.2, 1), \quad (h_2(0), h_2'(0)) = (0.3, 1),$$
$$m_1 = 2.5 \times 10^{-2}, \quad m_2 = 2 \times 10^{-2}, \quad u_0(x) = 0, \quad \lambda = 1.$$

We used $\Delta x = .001$, $\Delta t = 0.0005$, $\mu = .5$. See Figure 5.

Example 4.5. This example also has two particles. This time the particles are initially heading toward each other. The point is to see if the splitting scheme still
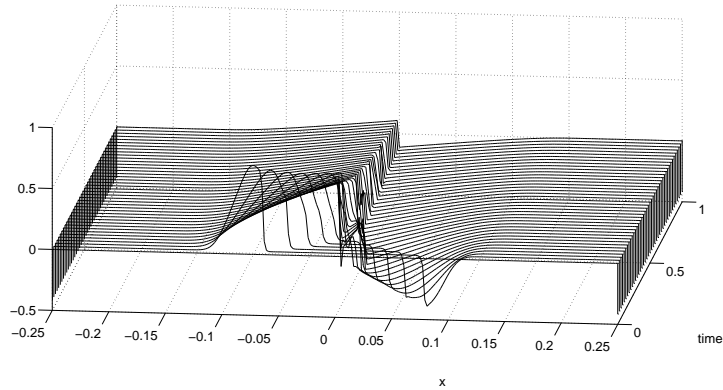
FIGURE 6.   Example 4.5. Fluid velocity. Two particles initially
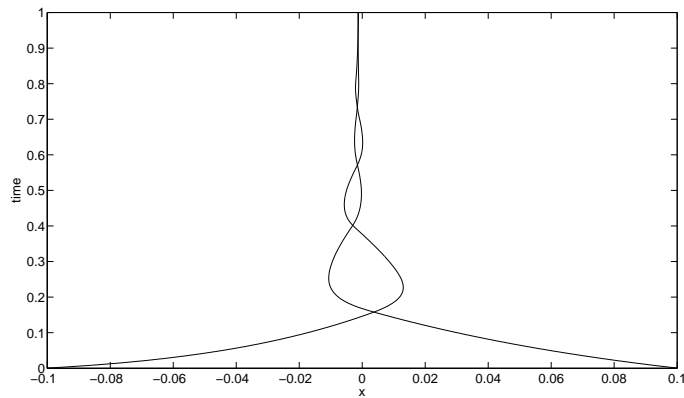headed toward each other.

FIGURE 7.   Example 4.5. Particle locations. Two particles ini-
tially headed toward each other.

gives reasonable results when the stencil shifts associated with the two particles are
in opposite directions. The data is

$$(4.5) \qquad \begin{aligned} (h_1(0), h_1'(0)) &= (.1, -1), \quad (h_2(0), h_2'(0)) = (-.1, 2) \\ m_1 &= .04, \quad m_2 = .02, \quad u_0(x) = 0, \quad \lambda = 1. \end{aligned}$$

We used $\Delta x = .002$, $\Delta t = 0.0005$, $\mu = .25$. See Figures 6 and 7.

5. Conclusion

We have presented a simple finite volume scheme for the fluid-particle model
(1.1). It is similar to those presented in [1] and [5], the main difference being our
method of handling the moving source term. We have shown that our single-particle
scheme enforces several stability properties, and that both the single-particle scheme
and the two-particle scheme preserve the total momentum.

We have not proven that our scheme converges to the unique entropy solution, but numerical experiments, a few of which are presented in Section 4, seem to indicate that this is the case. Although the scheme is only first order accurate, it captures interesting features of the particle motion, see Figures 5 and 7. Also, our numerical experiments indicate that the shock located at the particle position is resolved sharply, with no smearing. There is some smearing of other features away from the particle, as one would expect from a monotone scheme [11]. A future area of investigation could be to improve the accuracy away from the particle by incorporating standard high resolution methods for conservation laws.

Finally, although we have not established any stability results for our two-particle scheme, numerical experiments indicate that it is robust, and based on Example 4.4, it gives results very similar to the two-particle scheme in [5].

References

[1] N. Aguillon, F. Lagoutière, N. Seguin. Convergence of finite volume schemes for coupling between the inviscid Burgers equation and a particle. Preprint downloaded from http://arxiv.org/pdf/1412.0376.pdf.

[2] N. Aguillon. Riemann problem for a particle-fluid coupling. Preprint downloaded from http://arxiv.org/pdf/1312.2692.pdf.

[3] N. Aguillon. Numerical simulations of a fluid-particle coupling. *Finite Volumes for Complex Applications VII-Elliptic, Parabolic and Hyperbolic Problems Springer Proceedings in Mathematics & Statistics*, 78: 759–767, 2014.

[4] B. Andreianov, K. Karlsen, N. Risebro. A theory of L^1-dissipative solvers for scalar conservation laws with discontinuous flux. *Arch. Ration. Mech. Anal.*, 201:27–86, 2011.

[5] B. Andreianov, F. Lagoutière, N. Seguin, T. Takahashi. Small solids in an inviscid fluid. *Netw. Heterog. Media*, 5(3):385–404, 2010.

[6] B. Andreianov, F. Lagoutière, N. Seguin, T. Takahashi. Well-posedness for a one-dimensional fluid-particle interaction model. *SIAM J. Math. Anal.*, 46: 1030–1052, 2014.

[7] B. Andreianov, N. Seguin. Analysis of a Burgers equation with singular resonant source term and convergence of well-balanced schemes. *Discrete Contin. Dyn. Syst.*, 32(6):1939–1964, 2012.

[8] A. Harten. High Resolution schemes for hyperbolic conservation laws. *J. Comput. Phys.*, 49:357–393 , 1983.

[9] H. Holden, K. H. Karlsen, K.-A. Lie, N. H. Risebro. Splitting for Partial Differential Equations with Rough Solutions. European Math. Soc. Publishing House, Zurich, 2010.

[10] F. Lagoutière, N. Seguin, T. Takahashi. A simple 1D model of inviscid fluid-solid interaction. *J. Differential Equations*, 245: 3503–3544, 2008.

[11] R.J. Leveque. Finite volume methods for hyperbolic problems. Cambridge University Press, Cambridge, UK, 2002

[12] A. LeRoux. A numerical conception of entropy for quasi-linear equations. *Math. Comp.*, 31:848–872, 1977.